Electronic properties of quantum dots formed by magnetic double barriers in quantum wires

Hengyi Xu, T Heinzel and Igor Zozoulenko

Linköping University Post Print

N.B.: When citing this work, cite the original article.

Original Publication:

Hengyi Xu, T Heinzel and Igor Zozoulenko, Electronic properties of quantum dots formed by magnetic double barriers in quantum wires, 2011, Physical Review B. Condensed Matter and Materials Physics, (84), 3, 035319.

http://dx.doi.org/10.1103/PhysRevB.84.035319

Copyright: American Physical Society

http://www.aps.org/

Postprint available at: Linköping University Electronic Press

http://urn.kb.se/resolve?urn=urn:nbn:se:liu:diva-70345

Electronic properties of quantum dots formed by magnetic double barriers in quantum wires

Hengyi Xu and T. Heinzel*

Solid State Physics Laboratory, Heinrich-Heine-Universität, 40204 Düsseldorf, Germany

I. V. Zozoulenko

Solid State Electronics, Department of Science and Technology, Linköping University, 60174 Norrköping, Sweden (Received 29 April 2011; published 27 July 2011)

The transport through a quantum wire exposed to two magnetic spikes in series is modeled. We demonstrate that quantum dots can be formed this way which couple to the leads via magnetic barriers. Conceptually, all quantum dot states are accessible by transport experiments. The simulations show Breit-Wigner resonances in the closed regime, while Fano resonances appear as soon as one open transmission channel is present. The system allows one to tune the dot's confinement potential from subparabolic to superparabolic by experimentally accessible parameters.

DOI: 10.1103/PhysRevB.84.035319

Quantum dots (QDs) are quasi-zero-dimensional semiconducting systems in which the Fermi wavelength of the electrons is comparable to the spatial extension of the confinement.¹ Within the top-down approach, QDs are typically defined in a two-dimensional electron gas (2DEG) residing in a semiconductor heterostructure and can be tuned electrostatically by nanopatterned gate electrodes.² QD formation by magnetic confinement has been suggested as a potential alternative showing some fascinating and quite different phenomena.^{3–5} However, it has remained unclear how these systems can be implemented experimentally. Magnetic dots have been formed by using the fringe field of a ferromagnet on top of a semiconductor heterostructure.^{6,7} This concept leads to open dots such that Coulomb blockade is absent. This implies energy levels of large width and a poorly defined electron number in the dot. We are not aware of a scheme for strong, purely magnetic confinement. Strong confinement can, however, be achieved by combining electrostatic with magnetic fields, i.e., by exposing a quantum wire to a suitable magnetic field profile in the longitudinal direction.⁸ Weakly bound states have recently been observed on such a system, 9 while the strongly confined states have been conceptually inaccessible by transport experiments due to the diamagnetic shifts in the leads.

Here, we study theoretically QDs formed in a quantum wire which is exposed to two magnetic spikes, referred to as magnetic barriers, in series. We demonstrate that in this system, strong magnetic confinement can be achieved in a way that all states are experimentally accessible via transport measurements. Resonant tunneling dominates the transmission spectrum in the closed regime, while Fano resonances are found in the open regime. Furthermore, by changing the sample parameters, the shape of the confinement potential can be tuned. The conductance of two magnetic barriers in series which confine electrons in a quantum wire has been calculated earlier, 10-12 and these structures have also been suggested as spin filters. 13-16 However, in none of these papers were the properties of the QD itself or the character of the transmission resonances studied, while a comprehensive semiclassical theory of this structure has been published recently.¹⁷

Our model system is sketched in Fig. 1(a). It consists of a parabolic quantum wire (QWR) oriented in the x direction with the potential $V(y) = \frac{1}{2}m^*\omega_0^2y^2$ with a confinement strength $\omega_0 = 1.6 \times 10^{11} \text{ s}^{-1}$ and the effective electron mass for GaAs $m^* = 0.067m_e$. The QWR width in the y direction depends on the Fermi energy E_F , which can be tuned by a voltage applied to homogeneous gate electrode (not shown). The magnetic barriers are assumed to originate from a ferromagnetic stripe oriented across the QWR, i.e., in the y direction, which is magnetized in the x direction to the magnetization $\mu_0 M$ by a homogeneous, longitudinal external magnetic field \mathbf{B}^{ext} . The perpendicular (z) component of the fringe field $B_z(x)$ forms two magnetic barriers in series of opposite polarity and with a spacing L given by the width of the ferromagnetic stripe. This magnetic field profile can be written as z^{19}

PACS number(s): 73.63.Kv, 85.70.-w, 72.20.My

$$B_z(x) = \frac{\mu_0 M}{4\pi} \ln\left(\frac{A^+}{A^-}\right), \quad A^{\pm} = \frac{(x \pm L/2)^2 + d^2}{(x \pm L/2)^2 + (d+h)^2},$$
(1)

where h denotes the thickness of ferromagnetic film and d the distance of the QWR to the semiconductor surface. The main effect on the QWR is provided by $B_z(x)$, while the inplane components of **B** generate additional, small diamagnetic shifts which we neglect. Magnetic barrier peak fields of $B_x^{\max} \approx 0.57\,\mathrm{T}$ have been achieved experimentally this way. Furthermore, we assume $h=60\,\mathrm{nm}$ and $d=30\,\mathrm{nm}$. The effective g factor is set to zero and a spin degeneracy of 2 is assumed for all states.

Qualitatively, the QWR modes experience an x-dependent diamagnetic shift, and we denote their energies by $E_j(x)$, j = 1,2,..., given by²¹

$$E_j(x) = \left(j - \frac{1}{2}\right)\hbar\sqrt{\omega_0^2 + \omega_c^2(x)},\tag{2}$$

with the local cyclotron frequency $\omega_c(x) = eB_z(x)/m^*$. A symmetric double barrier emerges as sketched for the first mode in Fig. 1(a).

Quantitatively, the system is described by the effectivemass Hamiltonian $H = H_0 + V(y)$ where H_0 is the kinetic energy term. The magnetic field $B_z(x)$ enters via the vector

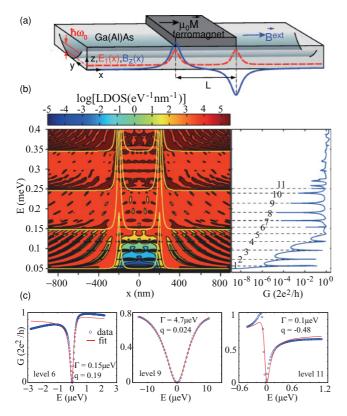


FIG. 1. (Color online) (a) Scheme of the system under study. The parabolic quantum wire resides in a semiconductor, e.g., a $GaAs/Al_xGa_{1-x}As$, heterostructure. A ferromagnetic stripe on top, magnetized in the x direction by an external magnetic field \mathbf{B}^{ext} , generates an inhomogeneous, perpendicular magnetic fringe field $B_z(x)$ (blue solid line) composed of two magnetic barriers below the edges of the ferromagnet. The red, dashed line indicates the corresponding energy of the wire mode with the lowest energy, $E_1(x)$. (b) Left: The LDOS as a function of E_F and x. Also shown (yellow full lines) are the mode energies $E_j(x)$. The magnetic barriers reside at $x=\pm 200$ nm. The corresponding two-terminal conductance is shown to the right. (c) Fits of selected resonances of (b) to the Fano formula.

potential as $\mathbf{A} = (-B_z(x)y, 0, 0)$ and the Peierls substitution in the momentum operator $\mathbf{p} \to \mathbf{p} + e\mathbf{A}$.

The resulting Schrödinger equation is solved numerically on a discretized lattice with a lattice constants a=2 nm in the x direction and b(E)=w(E)/128 where w(E) denotes the energy-dependent wire width. For all calculations, b was ≤ 5 nm. The discrete spatial coordinates at a given energy are thus x=ma (m=-500, -499,...,500) and y=nb (n=-64, -63,...,64), respectively. The tight-binding Hamiltonian of the system reads

$$H = \sum_{m} \left\{ \sum_{n} \epsilon_{0} c_{m,n}^{\dagger} c_{m,n} - t \{ c_{m,n}^{\dagger} c_{m,n+1} + e^{-iqw} c_{m,n}^{\dagger} c_{m+1,n} + \text{H.c.} \} \right\},$$
(3)

where ϵ_0 is the site energy, $t = \hbar^2/(2m^*a^2)$ is the hopping matrix element, and $c_{m,n}^{\dagger}(c_{m,n})$ denotes the creation (annihilation) operators, respectively, at site (m,n). Furthermore,

the phase factor is given by $q = \frac{e}{\hbar} \int_{x_i}^{x_{i+1}} B_z(x') dx'$. For transport calculations, the ends of the wire are connected to ideal semi-infinite leads. The two-terminal conductance G is calculated within the Landauer-Büttiker formalism and reads²¹

$$G = \frac{2e^2}{h} \sum_{\beta,\alpha=1}^{N} |t_{\beta\alpha}|^2,\tag{4}$$

where N is the number of propagating states in the leads, and $t_{\beta\alpha}$ is the transmission amplitude from incoming state α in the left lead (at x < -500a) to outgoing state β at x > 500a. It can be expressed in terms of the total Green's function **G** of the system as $t_{\beta\alpha} = i\hbar \sqrt{v_{\alpha}v_{\beta}} \mathbf{G}^{501,-501}$, where $\boldsymbol{G}^{501,-501}$ denotes the matrix $\langle 501|\boldsymbol{G}|-501\rangle$ with ± 501 corresponding to the position of the left and right lead, respectively, which takes into account the contributions of the initial and final states in the leads. We calculate $G^{501,-501}$ using the recursive Green's function technique in the hybrid space formulation.^{22,23} Afterward, we determine the surface Green's functions related to the left and right leads and the Green's function of the QWR separately and then link them at their interfaces. The local density of states (LDOS) as a function of the site $\mathbf{r} = (m,n)$ is related to the total Green's function in real space representation by LDOS($\mathbf{r}; E$) = $-\frac{1}{\pi}\text{Im}[\mathbf{G}(\mathbf{r},\mathbf{r};E)],$ where Im denotes the imaginary part.

We focus on a dot of length L = 400 nm in the low-energy regime where at most the lowest three modes of the leads are occupied. In Fig. 1(b), the LDOS as a function of xand E_F , integrated along the y direction, is shown for a magnetization of the ferromagnetic stripe of $\mu_0 M = 2 \text{ T}$. As expected from the simple picture sketched above, the diamagnetic shifts of the mode energies form an effective double barrier (yellow full lines) leading to quantized confinement. In the single-mode regime $(50 \,\mu\text{eV} < E_F < 150 \,\mu\text{eV})$, the mode spacing increases with increasing energy, reflecting the superparabolic confinement potential in longitudinal direction. The conductance correlates with the dot spectrum and shows resonant tunneling peaks; see the right part of Fig. 1(b). This indicates that the resonances are related to the energy spectrum of the dot and not to effects at the individual magnetic barriers as reported in Ref. 24 (note that the resonances investigated there have been obtained for hard wall wires and get suppressed in softer confinement potentials). As the second QWR mode becomes occupied, the character of the resonances switches from transmissive to reflective. These resonances are not necessarily symmetric and originate from interferences of the propagating states of the first QWR modes with bound states of the second or third QWR mode. They can thus be described by the Fano line shape²⁵

$$G(E_F) = \frac{2e^2}{h} \frac{1}{1+q^2} \frac{[q \pm \epsilon/2\Gamma]^2}{1+[\epsilon/2\Gamma]^2}.$$
 (5)

Here, Γ denotes the coupling of the bound state to the leads, $\epsilon = E_F - E_{\rm res}$ is the detuning from the resonance center $E_{\rm res}$, and q is the Fano parameter which is a measure of the phase difference between the two transmission channels the electron waves collect as they traverse the dot; i.e., $q = -\cot(\alpha - \delta)/2$ where α (δ) denotes the phase the wave

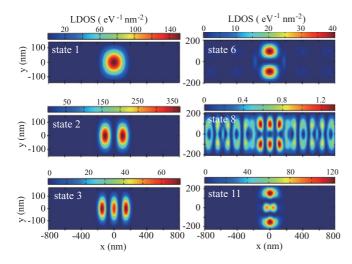


FIG. 2. (Color online) The LDOS of the bound states at the energies of selected resonances. The labels of the states refer to Fig. 1(b).

acquires while traversing the dot via the bound (free) state. For q=0, a symmetric dip is obtained. As |q| increases, the line shape becomes more asymmetric, and in the limit $|q| \to \infty$, Eq. (5) reduces to a Breit-Wigner resonance. For q>0 (q<0), the dip appears to the low (high) energy side of a peak.

Figure 1(c) depicts the fits of some resonances to Eq. (5). We find both positive and negative Fano parameters in the range |q| < 0.5, while the coupling of the states to the leads varies by up to a factor of 50. This behavior resembles that observed by Gores *et al.*²⁶ on an open, electrostatically defined QD, where, however, the Fano resonances showed larger asymmetries and a more homogeneous coupling.

The character of the bound states can be visualized with the help of spatially resolved LDOS plots at resonant energies; see Fig. 2. States belonging to the first wire mode have no node in the y direction, and the level index is given by the number of nodes in the x direction. State 6 (11) is the lowest energy state belonging to the second (third) wire mode. While sharp resonances originate from states well localized close to the center of the dot, transmission via more extended states, e.g., state 8, causes broad and almost symmetric resonances.

One potentially relevant feature of this system is the possibility to tune the confinement potential shape by experimentally controllable parameters, such as L, $B_z^{\rm max}$, or d. In general, the less the two magnetic barriers overlap, the steeper the effective confinement potential becomes. While changing L requires fabrication of several samples and d can be tuned parametrically by no more than about 25 nm, 27 $B_z^{\rm max}$ can be varied over wide ranges by changing $\mu_0 M$. In Fig. 3, the energies of the bound states in the closed regime are plotted as a function of the level index ℓ for various magnetizations. For $\mu_0 M < 5\,\mathrm{T}$, the level spacing increases with ℓ indicating superparabolic confinement, while for $\mu_0 M > 5\,\mathrm{T}$, the confinement is subparabolic. For the sample parameters chosen here, a magnetization of $5\,\mathrm{T}$

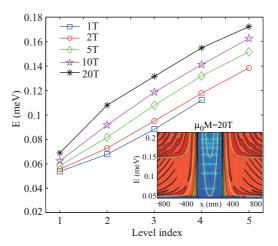


FIG. 3. (Color online) Parametric tuning of the confinement potential shape. Main figure: Energies of the quantum dot states in the closed regime as a function of the level index for various MB amplitudes. Inset: LDOS (E_F ,x) and $E_1(x)$ for a magnetization of 20 T, showing a subparabolic confinement effective potential.

represents an approximately parabolic confinement [the case $\mu_0 M = 2 \,\mathrm{T}$ is plotted in Fig. 1(b)]. The LDOS as a function of E_F and x for the strongest magnetization is shown in the inset of Fig. 3, where the subparabolicity is directly visible.

To summarize, we have shown that by exposing a quantum wire to two magnetic barriers in series, tunable quantum dots can be formed in which all discrete states are conceptually accessible by transport experiments. Such quantum dots may provide an alternative to conventional quantum dots defined by purely electrostatic confinement. They reveal the full variety of the possible forms of Fano resonances and show a large variation of the coupling of the dot states to the leads. Furthermore, the shape of the confinement potential can be changed continuously between subparabolic and superparabolic by experimentally accessible parameters. Quantum effects at magnetic double barriers in quantum wires have not been tested experimentally yet to the best of our knowledge. This is somewhat surprising, in particular considering that the necessary technology is essentially established. Several experiments on magnetic double barriers with submicron spacing have been performed in wide 2DEGs, 18,28-30 with the minimum 2DEG width of 1 μ m, reported in Ref. 28, which is probably too broad for detecting quantized states. The experimentally available magnetization is limited to about 3.75 T, such that the subparabolic potential regime lies outside experimental reach for the parameters we chose, but it should be possible to scale the system accordingly by a careful choice of the sample parameters. Alternatively, nonplanar 2DEGs may be used.³¹ Furthermore, magnetic confinement concepts have attained increased attention recently due to their potential application to graphene, 32,33 where electrostatic confinement is inhibited due to Klein tunneling.³⁴ It will be interesting to see whether the concept discussed here can be transferred to graphene nanoribbons.

H.X. and T.H. acknowledge financial support from Heinrich-Heine-Universität Düsseldorf.

- *thomas.heinzel@uni-duesseldorf.de
- ¹W. D. Heiss, editor, *Quantum Dots: A Doorway to Nanoscale Physics* (Springer, Berlin, 2005).
- ²L. P. Kouwenhoven, C. M. Marcus, P. L. McEuen, S. Tarucha, R. M. Westervelt, and N. S. Wingreen, in *Mesoscopic Electron Transport, Series E: Applied Sciences*, edited by L. L. Sohn, L. P. Kouwenhoven, and G. Schön (Kluwer, Dordrecht, The Netherlands, 1997).
- ³S. J. Lee, Phys. Rep. **394**, 1 (2004).
- ⁴H.-S. Sim, K. H. Ahn, K. J. Chang, G. Ihm, N. Kim, and S. J. Lee, Phys. Rev. Lett. **80**, 1501 (1998).
- ⁵J. Reijniers, F. M. Peeters, and A. Matulis, Phys. Rev. B **64**, 245314 (2001).
- ⁶D. Uzur, A. Nogaret, H. E. Beere, D. A. Ritchie, C. H. Marrows, and B. J. Hickey, Phys. Rev. B 69, 241301 (2004).
- ⁷A. Nogaret, J. Phys. Condens. Matter **22**, 253201 (2010).
- ⁸J. Reijniers, A. Matulis, K. Chang, F. M. Peeters, and P. Vasilopoulos, Europhys. Lett. **59**, 749 (2002).
- ⁹A. Tarasov, S. Hugger, H. Xu, M. Cerchez, T. Heinzel, I. V. Zozoulenko, U. Gasser-Szerer, D. Reuter, and A. D. Wieck, Phys. Rev. Lett. **104**, 186801 (2010).
- ¹⁰M. Governale and D. Boese, Appl. Phys. Lett. **77**, 3215 (2000).
- ¹¹H. Z. Xu and Y. Okada, Appl. Phys. Lett. **79**, 3119 (2001).
- ¹²F. Zhai, Y. Guo, and B.-L. Gu, Phys. Rev. B **66**, 125305 (2002).
- ¹³M.-W. Lu, L.-D. Zhang, and X.-H. Yan, Phys. Rev. B **66**, 224412 (2002).
- ¹⁴K. C. Seo, G. Ihm, K.-H. Ahn, and S. J. Lee, J. Appl. Phys. **95**, 7252 (2004).
- ¹⁵M. B. A. Jalil, J. Appl. Phys. **97**, 024507 (2005).
- ¹⁶F. Zhai and H. Q. Xu, Appl. Phys. Lett. **88**, 032502 (2006).
- ¹⁷G. Papp and F. M. Peeters, J. Appl. Phys. **107**, 063718 (2010).
- ¹⁸V. Kubrak, F. Rahman, B. L. Gallagher, P. C. Main, M. Henini, C. H. Marrows, and M. A. Howson, Appl. Phys. Lett. **74**, 2507 (1999).

- ¹⁹T. Vančura, T. Ihn, S. Broderick, K. Ensslin, W. Wegscheider, and M. Bichler, Phys. Rev. B 62, 5074 (2000).
- ²⁰S. Hugger, M. Cerchez, H. Xu, and T. Heinzel, Phys. Rev. B 76, 195308 (2007).
- ²¹S. Datta, *Electronic Transport in Mesoscopic Systems* (Cambridge University Press, Cambridge, UK, 1997).
- ²²I. V. Zozoulenko, F. A. Maao, and E. H. Hauge, Phys. Rev. B 53, 7975 (1996).
- ²³I. V. Zozoulenko, F. A. Maao, and E. H. Hauge, Phys. Rev. B 53, 7987 (1996).
- ²⁴H. Xu, T. Heinzel, M. Evaldsson, S. Ihnatsenka, and I. V. Zozoulenko, Phys. Rev. B 75, 205301 (2007).
- ²⁵U. Fano, Phys. Rev. **124**, 1866 (1961).
- ²⁶J. Gores, D. Goldhaber-Gordon, S. Heemeyer, M. A. Kastner, H. Shtrikman, D. Mahalu, and U. Meirav, Phys. Rev. B 62, 2188 (2001).
- ²⁷G. Salis, B. Graf, K. Ensslin, K. Campman, K. Maranowski, and A. C. Gossard, Phys. Rev. Lett. **79**, 5106 (1997).
- ²⁸S. Joo, J. Hong, K. Rhie, K. Y. Jung, K. H. Kim, S. U. Kim, B. C. Lee, W. H. Park, and K. Shin, J. Korean Phys. Soc. **48**, 642 (2006).
- ²⁹J. U. Bae, T. Y. Lin, Y. Yoon, S. J. Kim, J. P. Bird, A. Imre, W. Porod, and J. L. Reno, Appl. Phys. Lett. **91**, 022105 (2007).
- ³⁰T. Lin, K. Lim, A. M. Andrews, G. Strasser, and J. P. Bird, Appl. Phys. Lett. **97**, 063108 (2010).
- ³¹M. L. Leadbeater, C. L. Foden, J. H. Burroughes, M. Pepper, T. M. Burke, L. L. Wang, M. P. Grimshaw, and D. A. Ritchie, Phys. Rev. B 52, R8629 (1995).
- ³²A. DeMartino, L. Dell'Anna, and R. Egger, Phys. Rev. Lett. 98, 066802 (2007).
- ³³H. Xu, T. Heinzel, M. Evaldsson, and I. V. Zozoulenko, Phys. Rev. B 77, 245401 (2008).
- ³⁴A. H. C. Neto, F. Guinea, N. M. R. Peres, K. S. Novoselov, and A. K. Geim, Rev. Mod. Phys. **81**, 109 (2009).